LYMPHATIC RESEARCH AND BIOLOGY
Volume 00, Number 00, 2017

DOI: 10.1089/lrb.2016.0047

Original Article

Breast Cancer-Related Lymphedema: Differentiating Fat from Fluid Using Magnetic Resonance Imaging Segmentation

Yuka Sen, PhD,[1] Yi Qian, PhD,[1,*] Louise Koelmeyer, BAppSc (OT),[2] Robert Borotkanics, DrPH, MS, MPH,[3]
Robyn Ricketts, BAppSc (OT),[2] Helen Mackie, MBBS, FAFRM,[2] Thomas C. Lam, MBBS,[2]
Kevin Ho Shon, MBBS, BSc (Hons), MSc, PhD, FRANZCR,[2,4]
Hiroo Suami, MD, PhD,[2] and John Boyages, MBBS (Hons), FRANZCR, PhD[2,*]

Abstract

Background: Lymphedema is an iatrogenic complication after breast cancer treatment in which lymph fluid in the affected limb progresses to fat deposition and fibrosis that are amenable to liposuction treatment. Magnetic resonance imaging (MRI) for lymphedema can differentiate fat tissue from fluid, but estimating relative volumes remains problematic.

Methods and Results: Patients underwent routine bilateral arm MRI both before and after liposuction for advanced lymphedema. The threshold-based level set (TLS) segmentation method was applied to segment the geometric image data and to measure volumes of soft tissue (fat, muscle, and lymph fluid) and bone. Bioimpedance testing (L-Dex®) to detect extracellular fluid was also used. Volumes derived by using TLS or girth measurement were evaluated and showed consistent agreement, whereas L-Dex showed no significant reduction between pre- and postoperative measures. The percentage median volume difference between the affected and unaffected sides was 132.4% for girth measures compared with 137.2% for TLS ($p = 0.175$) preoperatively, and 99.8% and 98.5%, respectively ($p = 0.600$), postoperatively. MRI segmentation detected reductions in fat (median 52.6%, $p = 0.0163$) and lymph fluid (median 66%, $p = 0.094$), but the volumes of muscle and bone were relatively constant.

Conclusions: MRI imaging with TLS technology may be a useful tool to quantitatively measure fat tissue and fluid for patients with advanced lymphedema and may assist in the selection of eligible liposuction candidates at initial assessment and follow-up of patients who proceed with surgery.

Keywords: MRI, lymphedema, liposuction

Introduction

Breast cancer-related lymphedema (BCRL) occurs most commonly as a debilitating iatrogenic complication of axillary lymph node dissection, with an average incidence of 21.4% increasing to 50%–60% when axillary dissection is combined with radiation.[1–4] Lymphedema can cause pain, increase the risk of cellulitis, and limit a patient's activities of daily living, including bathing, dressing, grooming, and domestic tasks.[5]

With the staging treatment of axillary lymph nodes through surgery and sometimes additional radiation therapy, the remaining lymphatic structures become overloaded or blocked and their valves become incompetent, impeding their functionality. This failure spreads distally from the axilla to the peripheral lymph vessels, which, in turn, become dilated

Departments of [1]Biomedical Sciences and [2]Clinical Medicine, Faculty of Medicine and Health Sciences, Macquarie University, Sydney, Australia.
[3]Department of Biostatistics and Epidemiology, Faculty of Health and Environmental Sciences, Auckland University of Technology, Auckland, New Zealand.
[4]Macquarie Medical Imaging, Macquarie University Hospital, Macquarie University, Sydney, Australia.
*These authors contributed equally to this work.

and nonfunctional.[6] Protein-rich exudate accumulates in the dependent tissue, leading to swelling of the ipsilateral arm.[7]

BCRL is commonly staged according to clinical presentation.[8] Early stage (International Society of Lymphology [ISL] Stage 1) BCRL is characterized by accumulation of lymph fluid in the interstitial tissue with no fibrosis. At this stage, the swelling in the extremities can be reversible and relieved via prolonged elevation of the affected extremity. Advancing BCRL stage and increasing tissue volume leads to fat deposition followed by fibrosis in the affected limb.[6,9,10]

Brorson et al. developed liposuction protocols for advanced lymphedema,[11–13] the rationale being that the associated swelling is not due solely to lymphatic fluid but also to accumulating adipose tissue[6,14] and sometimes fibrosis.[15] Liposuction significantly reduces excess limb volume[11,15,16] for patients with advanced upper or lower extremity lymphedema,[11,13,17,18] with ongoing reduction maintained by continuous compression garment use.[15,16,19] The pitting test, part of the physical examination to determine the level of fluid accumulation, is an easy screening tool to determine eligibility for liposuction; however, it may be associated with inter-observer variation. Validation with other techniques such as magnetic resonance imaging (MRI) is useful.[20]

Successful management of BCRL relies on early diagnosis and appropriate intervention by using sensitive measurement techniques. Upper limb volume can be measured via circumferential limb girth, water displacement, and perometry, and bioimpedance spectroscopy has been used to determine the extent of extracellular fluid.[21] We have previously reported that water displacement during limb immersion, considered the standard benchmark, correlates highly to volume measurements derived from a truncated cone formula.[22] However, the water displacement method and derived volumes are limited, as they are unable to distinguish changes in muscle, adipose tissue, or extracellular fluid volume. Nor are they able to identify localized areas of swelling. Further, water displacement is rarely performed, as it is cumbersome and time-consuming in clinical settings.

Several imaging techniques have been used for qualitative assessment of lymphedema. Lymphoscintigraphy is a standard diagnostic imaging modality in which a radiotracer is used to demonstrate the lymphatic system in the affected limb. The disadvantage of lymphoscintigraphy is poor spatial resolution, but it does allow an understanding of the extent of drainage to the axillary lymph nodes. Poor drainage is manifested through the presence of dermal backflow, which indicates recirculation of lymphatic fluid rather than normal drainage to the regional nodes and eventually into the venous system. A lymphoscintigram can also show tracer uptake in regional lymph nodes, indicating proper functioning, as well as drainage bypassing the regional nodes, for example, to the internal mammary chain or opposite axilla. This test is useful, particularly as a tool in lymph node transfer to determine which lymph node to harvest to avoid compromising the lymphatic system at the donor site.[23]

Indocyanine green (ICG) fluorescence lymphangiography is an emerging imaging technique using near infrared technology. This real-time outpatient or intraoperative procedure can evaluate the superficial lymphatics up to 15 mm below the surface of the skin and again serves as a useful baseline before deciding on surgical intervention. Classification of the severity of lymphedema based on fluorescence lymphographic images has been reported.[24] Both ICG lymphography and lymphoscintigraphy evaluate function, but their usefulness after surgical intervention may be limited. Further, no modalities, including conventional MRI, can correlate the proportion of lymphatic fluid versus fat in an affected limb.

MRI has had limited usage in patients with advanced lymphedema, largely because of cost and discomfort, and partly because of limitations in analyzing the imaging data. However, the soft-tissue contrast provided by MRI enables accurate characterization of changes in both affected and unaffected limbs. Contrast-enhanced MR lymphography can be used to visualize the lymphatics, but again this technique remains experimental and is more invasive for the patient.[25]

MRI imaging has made it possible to visualize and take three-dimensional (3D) measurements of tissue within the limbs, allowing reconstruction of patient-specific bone, muscle, fat, and lymphatic fluid. However, due to complications such as generation of random noise, intensity inhomogeneity, and partial volume effect, segmentation of soft tissue containing lymphatic fluid in patients with BCRL is a highly challenging task. For example, it is difficult to accurately separate blood from lymph liquid by using noncontrast MRI. To date, there have been no reports focusing on the use of 3D MRI reconstruction of bone, muscle, adipose tissue, and lymphatic fluid to measure associated volumes within limbs for the diagnosis and evaluation of BCRL. In this article, preoperative and postoperative MRI data from five patients with BCRL undergoing liposuction were used for a pilot analysis. The threshold-based level set (TLS) segmentation method was used to segment data obtained from these images.[26,27]

Materials and Methods

Patient data

Five upper limb lymphedema patients with MRI scans before and after liposuction surgery were selected from the records of patients attending the Advanced Lymphedema Assessment Clinic (ALAC) at Macquarie University Hospital. Patients attending the ALAC were evaluated after having provided informed consent. The clinical and imaging protocols were approved by the Macquarie University Human Research Ethics Committee (Ref.: 5201300315).

Eligibility criteria for liposuction were (1) unilateral, nonpitting primary or secondary advanced ISL stage II or III lymphedema; (2) limb volume difference greater than 25% (calculated using truncated-cone method); and (3) decongestive lymphatic therapy provided no further volume reductions.[6,13]

MRI protocols

Upper limb MRI was performed in each participant by using a clinical 3T MRI machine (3.0T Siemens Verio). The images were obtained with the patient supine and head-first into the gantry. The arm of interest is at the patient's side, and surface coils are positioned to image the arm from the proximal humerus to the distal radius.

The image data obtained were exported into DICOM format, with all images measured on a high-field strength system at the Macquarie University Hospital at Macquarie Medical

Imaging (MMI). Scans covered the area between the proximal humerus at the shoulder joint to the distal radius at the wrist joint in both the affected and unaffected limbs of each patient. The upper extremity of the patient was scanned in three separate blocks with 40 images per block by using 5 mm distance between images. The image resolution was 512×512 on each slide. The study utilized a spine coil in combination with an anterior phase array coil. A standardized protocol used for all participants included: axial short tau inversion recovery (STIR) time of repetition (TR) 7000 mseconds, time to echo (TE) 35 mseconds, time of inversion (TI) 215 mseconds, and axial T1 fast spine echo (FSE) TR 600 mseconds, TE 9.5 mseconds. Slices of continuous thickness were used to segment and reconstruct the 3D geometry of bone, muscle, fat, and lymphatic fluid. The time of the second MRI varied between patients because of factors such as cost and accessibility to the clinic, as some were from outside our state of NSW.

Segmentation methods

In this article, we used our previously developed segmentation algorithm TLS.[27] This method is based on the Geodesic Active Contours (GAC) model[28] and Chan-Vese (CV) model,[26] integrating both region and boundary information to segment the components of the enlarged limb affected by lymphedema through use of a global threshold and gradient magnitude to form the speed function.

We used geometric information of the image data to eliminate overlap in the three blocks of images to form a 3D image of the whole limb. Hence, at the preprocessing stage, there was no longer any overlap, eliminating this potential concern of the segmentation process. The initial threshold is calculated by using the result of the CV model and is then iteratively updated throughout the process of segmentation.[26] On reaching the target tissue boundary, the variation of the threshold declines because of the contrast between target tissue and surrounding tissue intensities, and the process stops. This algorithm can be implemented in an automatic or semi-automatic form depending on the complexity of the tissue shape.

The TLS method combines the GAC and the CV model[26] together within the level set framework.[27]

Under the level set scheme, the contour deforms by the function; $\frac{\partial \Gamma(t)}{\partial t} + F|\nabla\varphi| = 0$, with an embedded surface $\Gamma(t)$ represented as the zero level set of φ by $\Gamma(t) = \{x, y \in R | \varphi(x, y, t) = 0\}$. F is a function for speed, which drives the $\Gamma(t)$ surface evolution in the normal direction. It is clear that F directly impacts the quality of medical image segmentation. The associated evolution equation in the level set framework is as follows:

$$\frac{\partial \varphi}{\partial t} = |\nabla\varphi| \left[\alpha(I - T) + \beta div\left(g \frac{\nabla\varphi}{|\nabla\varphi|} \right) \right], \tag{1}$$

where I represents the image to be segmented, T represents the intensity threshold, g represents the image gradient,[27] $div\left(\frac{\nabla\varphi}{|\nabla\varphi|}\right)$ represents the curvature, α represents the image propagation constant, and β represents the spatial modifier constant for the curvature $div\left(\frac{\nabla\varphi}{|\nabla\varphi|}\right)$, α, and β weight the relative influence of each of these terms on the movement of the surface contour.

According to the theory of confidence intervals, the lower bound threshold of the segmenting tissue can be defined by:

$$T_i = \mu_a - k_i \sigma_a \quad i \geq 0. \tag{2}$$

The threshold T is the difference between the mean of the contour of the segmenting tissue (μ_α) and k times its standard deviation (σ_α). The intensities of the segmenting tissue and its background regions are different. The lowest

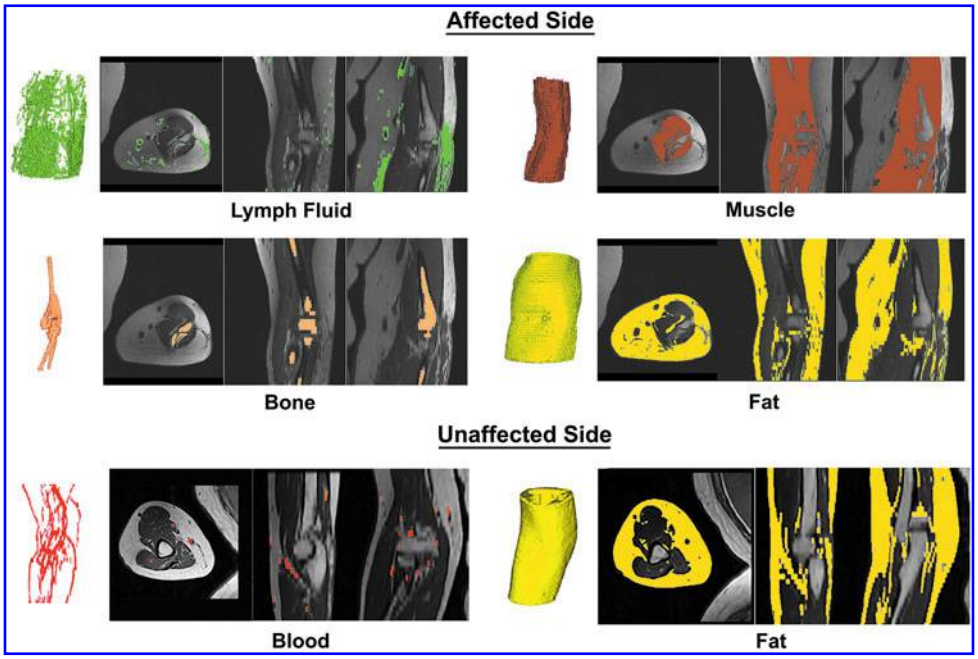

FIG. 1. Segmentation of limb components.

Table 1. Patient Demographics

Patient	*1*	*2*	*3*	*4*	*5*
Patient factors					
Age at liposuction (years)	64.6	71.6	55.8	73.4	55.8
Height (m)	1.65	1.58	1.63	1.70	1.60
Preoperative weight	68	94	60	84	79
Postoperative weight	66	99	63	86	72
Preoperative body mass index	25.0	37.7	22.6	29.1	30.9
Postoperative body mass index	24.2	39.7	23.7	29.8	28.1
Hand dominance	Right	Right	Right	Right	Left
Tumor and treatment factors					
Year of diagnosis of breast cancer	1997	2012	2007	2008	2002
Age at diagnosis of breast cancer	48	69	49	67	44
Previous radiation therapy	No	Yes	Yes	Yes	Yes
Previous chemotherapy	No	Yes	Yes	Yes	Yes
Lymphedema factors					
Year of diagnosis	1997	2013	2007	2008	2002
Duration of lymphedema (years)	16.7	1.4	6.6	6.0	11.8
Time to second MRI from surgery (months)	6.1	12.1	5.2	11.2	5.3
Affected side	Right	Right	Left	Left	Left

MRI, magnetic resonance imaging.

intensity threshold of the segmenting tissue is the same as the highest intensity threshold of the background. Thus, $\mu_b + k_b\sigma_b = \mu_a - k_a\sigma_a$ would apply. The confidence level for both the segmenting tissue and background is considered the same; $k_b = k_a = k$. Therefore, k can be described as:

$$k = \frac{\mu_a - \mu_b}{\sigma_a + \sigma_b}. \quad (3)$$

We utilized the CV model method to perform an initial segmentation. From the segmentation results, the initial k_o can be calculated by Equation 3. The initial T_o can subsequently be found by using Equation 2. The initial zero level set is a cylinder surface, constructed via the manual input of an initial seed on the image for each tissue type. These parameter settings have been validated in our previous publication.[27]

Table 2. Comparison of Girth-Derived or Magnetic Resonance Imaging-Derived Total Limb Volume

Patient	*1*	*2*	*3*	*4*	*5*	
Girth-derived volume (mL)						
Preoperative						Median
Affected arm	2666	5468	2909	3240	4279	3240
Unaffected arm	2042	4104	2197	2600	2903	2600
Affected/unaffected (%)	130.6	133.2	132.4	124.6	147.4	132.4
Postoperative						
Affected arm	2157	3258	2107	3324	2940	2940
Unaffected arm	2229	3788	2112	3219	2724	2724
Affected/unaffected (%)	96.8	86.0	99.8	103.3	107.9	99.8
MRI derived volume (mL)						
Preoperative						
Affected arm	2250	3691	2472	2941	3183	2941
Unaffected arm	1641	2619	1874	2189	2073	2073
Affected/unaffected (%)	137.2	140.9	131.9	134.4	153.5	137.2
Postoperative						
Affected arm	1557	2636	1635	2144	1885	1885
Unaffected arm	1667	3227	1659	1936	1913	1913
Affected/unaffected	93.4	81.7	98.5	110.7	98.5	98.5
L-Dex measures						
Preoperative	18.0	78.7	32.8	70.6	31.8	32.8
Postoperative	17.4	42.5	38.4	27.9	28.5	28.5
Change in L-Dex (%)	−3.3	−46.0	17.1	−60.5	−10.4	−10.4

MRI, magnetic resonance imaging.

Segmentation procedure

The dominant signal intensities of different tissues on T1-weighted MRI images indicated that fluid shows low signal intensity (black), muscle shows intermediate signal intensity (gray), and bone and fat show high signal intensity (white). Therefore, the de-noised and bias-corrected T1-weighted images were utilized in segmenting the bone, muscle, and fat. Considering the MRI measurement in this study was non-contrast MRI, it was difficult to accurately separate blood from lymph liquid. Therefore, when we segmented the blood volume of the unaffected arm, we assumed that the volume of blood (and small amounts of normal lymph) was the same in both arms. The volume of lymph fluid in the affected arm was calculated by deducting the volume of blood measured in the unaffected arm.

The signal intensities on fat-suppressed T2-weighted STIR MRI images indicated that fluid shows high signal intensity (white) and muscle or fat shows low signal intensity (black). The lymph fluid was segmented on fat-suppressed T2-weighted STIR images. The bone, muscle, fat tissue, and liquid were then reconstructed in 3D. Figure 1 depicts the results of 3D imaging of bone, muscle, fat, blood, and lymphatic fluid from patient 1. The 3D geometries of bone, muscle, fat, blood, and lymph fluid were colored beige, brown, yellow, red, and green, respectively. Two-dimensional axial, sagittal, and coronal sections were also created.

Our previously developed program based on the TLS algorithm was used in the segmentation process for all five cases. The process was fully automated once we initialed a segmentation seed on the targeted image (fat, muscle, bone, or lymphatic fluid) that needed to be measured.[25]

Limb volume measurement

The limb volume was calculated by using 4 cm truncated cone circumferential measurements.[29] A measuring board was used, with the patient seated and the arm in horizontal abduction, hand pronated. Measurements commenced at the ulnar styloid. Individual limb volume was calculated, as well as the total volume and percentage difference between the affected and unaffected limbs.[22,29] The results of limb volume using girth calculations was compared with the limb volume calculated by the 3D segmentation of MRI images.

Bioimpedance spectroscopy (L-Dex). Measurements were taken supine by using bioimpedance spectroscopy (L-Dex; Impedimed, Carlsbad, CA) to calculate extracellular fluid in a unilateral limb using low voltage electrical current. The spectroscopy readings are an impedance ratio comparing unaffected and affected limb, with the unaffected limb acting as a patient-specific internal control.[30] The skin was cleaned with alcohol swabs and electrodes placed according to the manufacturer's recommendations. A normal (no-lymphedema) L-Dex score reading range is between −10 and 10.[31] This is a standard technique used for patients with lymphoedema to indicate the presence of extracellular fluid.

Results

The mean duration of lymphedema at the time of surgery was 8.5 years (range 1.4–16.7 years). Table 1 shows the

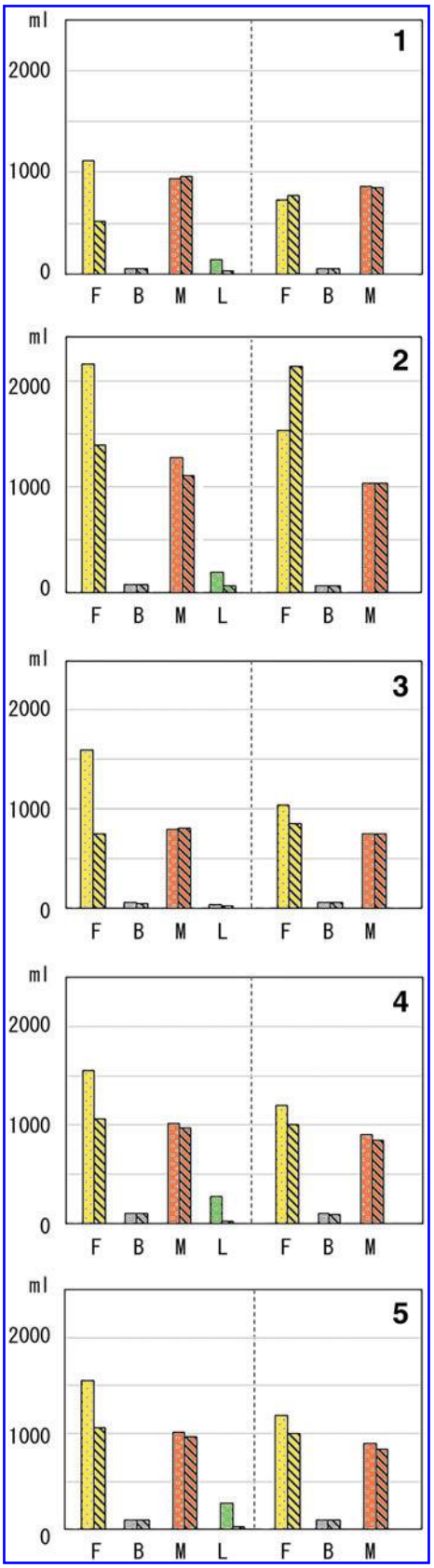

FIG. 2. Pre- and postoperative volumes of fat (F), bone (B), and muscle (M) ± lymph fluid (L) of affected arm (*left panel*) or unaffected arm (*right panel*). *Dotted bars* indicate preoperative, and *hashed bars* indicate postoperative.

Table 3. Changes in Magnetic Resonance Imaging Volume of Fat, Bone, Muscle, and Lymph Fluid after Liposuction

Patient	*1*	*2*	*3*	*4*	*5*	
Preoperative MRI volume (mL)						
Affected arm						Median
Fat	1119	2162	1593	1554	1712	1593
Bone	50	67	50	98	59	59
Muscle	942	1275	800	1013	959	959
Lymph fluid	138	186	29	276	453	186
Total volume	2250	3691	2472	2941	3183	2941
Unaffected arm						
Fat	725	1531	1042	1194	1103	1103
Bone	53	60	48	96	57	57
Muscle	863	1028	784	898	913	898
Lymph fluid	0	0	0	0	0	0
Total volume	1641	2619	1874	2189	2073	2079
Postoperative MRI volume (mL)						
Affected arm						
Fat	516	1395	755	1064	786	786
Bone	50	71	50	95	52	52
Muscle	962	1107	810	965	851	962
Lymph fluid	29	63	19	20	196	29
Total volume	1557	2636	1635	2144	1885	1885
Unaffected arm						
Fat	788	2133	856	1006	996	996
Bone	41	63	57	91	57	57
Muscle	839	1031	746	839	859	839
Lymph fluid	0	0	0	0	0	0
Total volume	1667	3227	1659	1936	1913	1913
Affected arm						
Change in lymph fluid (%)	–79.2	–66.0	–32.9	–92.8	–56.8	–66.0
Change in fat (%)	–53.9	–35.5	–52.6	–31.5	–54.1	–52.6
Change in muscle (%)	2.1	–13.1	1.3	–4.7	–11.3	–4.7
Change in bone (%)	–0.58	4.91	–0.82	–3.21	–11.38	–0.82

patient, tumor, treatment, and lymphedema characteristics both before and after liposuction. Most patients developed their lymphedema within the first year after breast cancer surgery. Most patients lost some weight after their surgery, but patients 2 and 3 gained 5 and 3 kg, respectively (Table 1).

Table 2 compares pre- and postoperative limb volumes derived from traditional girth measures to those derived using TLS segmentation of the MRI. The percentage median preoperative volume difference between the affected and unaffected sides was 132.4% (interquartile range (IQR): 130.6–133.2) for girth measures compared with 137.2% (IQR: 134.4–140.9) for TLS. The percentage difference between girth measures and TLS was not statistically significant (Mann–Whitney U test: $z = 1.358$, $p = 0.175$). The percentage median postoperative volume difference between the affected and unaffected sides was 99.8% (IQR: 96.8–103.3) for girth measures compared with 98.5% (IQR: 93.4–98.5) for TLS (Mann–Whitney U test: $z = 0.524$, $p = 0.600$). Although these relative differences were not significant, individual girth-derived volume calculations were uniformly higher than MRI-derived volume calculations.

L-Dex measures, measuring extracellular fluid, increased for patient 3, but decreased for all other patients and did not demonstrate a statistically significant difference overall both before and after liposuction (Mann–Whitney U test: $z = 0.940$; $p = 0.347$. The % median change in L-Dex before and after surgery was −10.4%, but ranged widely from +52.2% to −60.5% (Table 2).

The volumes of bone, fat, muscle, and fluid for all five patients derived from the MRI are shown in Figure 2 and Table 3. The median volume was higher for fat, muscle, and lymph fluid, but not bone, for the affected limb compared with the unaffected limb. In contrast to L-Dex, the results indicated a reduction in lymph fluid in the affected limb across all patients, but this difference was just outside statistical significance (Mann–Whitney U test: $z = 1.676$, $p = 0.094$) (Table 3). Aside from alterations in lymph fluid, the fat volume in the affected limb was also observed to decline at the follow-up observation and this difference was statistically significant (Mann–Whitney U test: $z = 2.402$, $p = 0.0163$). The overall volume also significantly decreased, at a statistically significant decline (Mann–Whitney U test: $z = 2.193$, $p = 0.0283$). As expected, there were no statistically significant differences pre- and postsurgery in the unaffected limb.

Discussion

This study found that MRI segmentation may be an appropriate method to help clinicians advise patients on the relative components of fat, fluid, bone, and muscle in a limb affected by lymphedema, guide decisions about surgical intervention, and inform outcomes after surgery. To our

knowledge, this technique has not been used before for patients with lymphedema. MRI segmentation identified reductions in fat (52.6%) and lymph fluid (66%), whereas L-Dex, a more commonly used and less expensive measure of extracellular fluid, showed no significant reduction in pre- versus postoperative measures in this surgical setting.[32]

We believe that the almost identical total reductions in volume both before and after liposuction verifies the consistency of each measurement technique and that MRI segmentation complements the validated girth measure technique while providing the clinician with a quantitative and visual understanding of the sub-components of the enlarged limb.[11] For example, it has been previously demonstrated by using dual energy X-ray absorptiometry (DXA) that muscle mass (not fat alone) increases in an enlarged limb, simply because the patient is carrying more weight every day.[14]

Advancement in microsurgical techniques for lymphoedema has resulted in the need for high-quality lymphatic imaging techniques to help choose the correct procedure and assist in evaluation of postsurgical outcome. Previously, lymphoscintigraphy was the gold standard,[33–35] but this has a low spatial resolution. Injection of ionizing radiation tracer into the web space in the hand or foot can be uncomfortable for patients.[36,37] It is also unable to quantify the proportion of abnormal fat deposition in an affected limb.

Another challenge facing patients and clinicians is having accurate information to determine the appropriate surgical procedure. For example, we have found that MRI may show areas of fatty deposition to help guide liposuction, and other procedures such as indocyanine green (ICG) lymphography help identify whether superficial lymphatics are still patent or are affected by significant dermal backflow.[24] Although bioimpedance is helpful for patients with early stage lymphedema, it is probably not ideal for advanced stage 2 or stage 3 lymphedema in which fatty deposition occurs. L-Dex values varied markedly from the normal upper limit of 10, ranging in value from 18.0 in patient 1 to 78.7 for patient 2, with no significant difference between pre- and postoperative values. In contrast, the MRI segmentation method was more accurate, with clinically significant reductions in both fat and lymph fluid detected.

Limitations

As mentioned earlier, three separate image blocks were taken of each affected and unaffected arm, due to the scanning size limitation of the MRI machine. Although we used our segmentation software to delete areas of image overlap, there was still some uncertainty at the top and bottom of the image scanned before and after treatment for the same patient. It is for this reason that bone volume differed both before and after treatment (Table 3). There was some variation in girth and MRI volumes for the unaffected arm, which did not completely parallel with postliposuction weight changes for the individual patient. Girth obviously reflects a combination of bone, fat, fluid, and muscle, and weight changes may not necessarily result in consistent fat deposition in the unaffected arm. Further, previous studies of cosmetic liposuction have found that liposuction in one area can result in compensatory fat depositions elsewhere. This complexity may be biological and/or reflect the lack of precision in comparing MRI volumes with girth measures, necessitating further study in a larger number of patients.[38] For future patients, we will standardize these points of uncertainty by placing a standard mark on the patient by using anatomical landmarks and measures.

Conclusions

We consider it possible to fully utilize a patient's MRI information by applying TLS segmentation technology to quantitatively measure and reconstruct 3D fluid, fat, muscle, adipose, and bone. We believe this will be a useful method to objectively evaluate changes, particularly in lymph fluid volume, after procedures such as lymphovenous anastomosis and lymph node transfer.

Acknowledgments

The authors would like to acknowledge the staff of Macquarie Medical Imaging (MMI) who performed the MRIs at a subsidized cost and the staff supporting the Advanced Lymphedema Assessment Clinic (ALAC).

Author Disclosure Statement

No competing financial interests exist.

References

1. DiSipio T, Rye S, Newman B, Hayes S. Incidence of unilateral arm lymphoedema after breast cancer: A systematic review and meta-analysis. Lancet Oncol 2013; 14:500–515.
2. Petrek JA, Heelan MC. Incidence of breast carcinoma-related lymphedema. Cancer 1998; 83:2776–2781.
3. Petrek JA, Senie RT, Peters M, Rosen PP. Lymphedema in a cohort of breast carcinoma survivors 20 years after diagnosis. Cancer 2001; 92:1368–1377.
4. Zissiadis Y, Langlands AO, Barraclough B, Boyages J. Breast conservation: Long-term results from Westmead Hospital. Aust N Z J Surg 1997; 67:313–319.
5. Boyages J, Kalfa S, Xu Y, Koelmeyer L, Mackie H, Viveros H, Taksa L, Gollan P. Worse and worse off: The impact of lymphedema on work and career after breast cancer. Springerplus 2016; 5:1–8.
6. Brorson H, Ohlin K, Olsson G, Nilsson M. Adipose tissue dominates chronic arm lymphedema following breast cancer: An analysis using volume rendered CT images. Lymphat Res Biol 2006; 4:199–210.
7. Donahue MJ, Donahue PC, Rane S, Thompson CR, Strother MK, Scott AO, Smith SA. Assessment of lymphatic impairment and interstitial protein accumulation in patients with breast cancer treatment-related lymphedema using CEST MRI. Magn Reson Med 2016; 75:345–355.
8. The diagnosis and treatment of peripheral lymphedema: 2013 Consensus Document of the International Society of Lymphology. Lymphology 2013; 46:1–11.
9. Jager G, Doller W, Roth R. Quality-of-life and body image impairments in patients with lymphedema. Lymphology 2006; 39:193–200.
10. Lawenda BD, Mondry TE, Johnstone PA. Lymphedema: A primer on the identification and management of a chronic condition in oncologic treatment. CA Cancer J Clin 2009; 59:8–24.
11. Brorson H. Liposuction gives complete reduction of chronic large arm lymphedema after breast cancer. Acta Oncol 2000; 39:407–420.

12. Damstra RJ, Voesten HG, Klinkert P, Brorson H. Circumferential suction-assisted lipectomy for lymphoedema after surgery for breast cancer. Br J Surg 2009; 96:859–864.
13. Schaverien MV, Munro KJ, Baker PA, Munnoch DA. Liposuction for chronic lymphoedema of the upper limb: 5 years of experience. J Plast Reconstr Aesthet Surg 2012; 65:935–942.
14. Brorson H, Ohlin K, Olsson G, Karlsson MK. Breast cancer-related chronic arm lymphedema is associated with excess adipose and muscle tissue. Lymphat Res Biol 2009; 7:3–10.
15. Brorson H. From lymph to fat: Liposuction as a treatment for complete reduction of lymphedema. Int J Low Extrem Wounds 2012; 11:10–19.
16. Brorson H. From lymph to fat: Complete reduction of lymphoedema. Phlebology 2010; 25 Suppl 1:52–63.
17. Brorson H. Liposuction in arm lymphedema treatment. Scand J Surg 2003; 92:287–295.
18. Brorson H, Ohlin K, Svensson B, Åberg M, Svensson H. Liposuction normalizes elephantiasis of the leg: A prospective study with an eight-year follow-up. American Association of Plastic Surgeons 91st Annual Meeting San Francisco, CA; 2012: 14–17.
19. Brorson H, Svensson H. Liposuction combined with controlled compression therapy reduces arm lymphedema more effectively than controlled compression therapy alone. Plast Reconstr Surg 1998; 102:1058–1067; discussion 68.
20. Sanderson J, Tuttle N, Box R, Reul-Hirche H, Laakso E-L. The pitting test: An investigation of an unstandardized assessment of lymphedema. Lymphology 2015; 48:175–183.
21. Ward LC, Czerniec S, Kilbreath SL. Operational equivalence of bioimpedance indices and perometry for the assessment of unilateral arm lymphedema. Lymphat Res Biol 2009; 7:81–85.
22. Taylor R, Jayasinghe UW, Koelmeyer L, Ung O, Boyages J. Reliability and validity of arm volume measurements for assessment of lymphedema. Phys Ther 2006; 86:205–214.
23. Modi S, Stanton AW, Mortimer PS, Levick JR. Clinical assessment of human lymph flow using removal rate constants of interstitial macromolecules: A critical review of lymphoscintigraphy. Lymphat Res Biol 2007; 5:183–202.
24. Suami H, Chang D, Skoracki R, Yamada K, Kimata Y. Using indocyanine green fluorescent lymphography to demonstrate lymphatic architecture. J Lymphoedema 2012; 7:25–29.
25. Sevick-Muraca EM, Kwon S, Rasmussen JC. Emerging lymphatic imaging technologies for mouse and man. J Clin Invest 2014; 124:905–914.
26. Chan TF, Vese LA. Active contours without edges. IEEE Trans Image Process 2001; 10:266–277.
27. Sen Y, Qian Y, Avolio A, Morgan M. Development of image segmentation methods for intracranial aneurysms. Comput Math Methods Med 2013; 2013:715325.
28. Caselles V, Kimmel R, Sapiro G. Geodesic active contours. Int J Comput Vis 1997; 22:61–79.
29. Brorson H, Hoijer P. Standardised measurements used to order compression garments can be used to calculate arm volumes to evaluate lymphoedema treatment. J Plast Surg Hand Surg 2012; 46:410–415.
30. Ward LC, Essex T, Cornish BH. Determination of Cole parameters in multiple frequency bioelectrical impedance analysis using only the measurement of impedances. Physiol Meas 2006; 27:839–850.
31. Fu MR, Cleland CM, Guth AA, Kayal M, Haber J, Cartwright F, Kleinman R, Kang Y, Scagliola J, Axelrod D. L-dex ratio in detecting breast cancer-related lymphedema: Reliability, sensitivity, and specificity. Lymphology 2013; 46:85–96.
32. Boyages J, Kastanias K, Koelmeyer LA, Winch CJ, Lam TC, Sherman KA, Munnoch DA, Brorson H, Ngo QD, Heydon-White A, Magnussen JS, Mackie H. Liposuction for advanced lymphedema: A multidisciplinary approach for complete reduction of arm and leg swelling. Ann Surg Oncol 2015; 22:1263–1270.
33. Campisi C, Boccardo F. Microsurgical techniques for lymphedema treatment: Derivative lymphatic-venous microsurgery. World J Surg 2004; 28:609–613.
34. Matsubara S, Sakuda H, Nakaema M, Kuniyoshi Y. Long-term results of microscopic lymphatic vessel-isolated vein anastomosis for secondary lymphedema of the lower extremities. Surg Today 2006; 36:859–864.
35. Weiss M, Baumeister RG, Hahn K. Dynamic lymph flow imaging in patients with oedema of the lower limb for evaluation of the functional outcome after autologous lymph vessel transplantation: An 8 year follow-up study. Eur J Nucl Med Mol Imaging 2003; 30:202–206.
36. Weissleder H, Weissleder R. Lymphedema: Evaluation of qualitative and quantitative lymphoscintigraphy in 238 patients. Radiology 1988; 167:729–735.
37. Williams WH, Witte CL, Witte MH, McNeill GC. Radionuclide lymphangioscintigraphy in the evaluation of peripheral lymphedema. Clin Nucl Med 2000; 25:451–464.
38. Seretis K, Goulis DG, Koliakos G, Demiri E. Short and long-term effects of abdominal lipectomy on weight and fat mass in females: A systematic review. Obes Surg 2015; 25:1950–1958.

Address correspondence to:
John Boyages, MBBS (Hons), FRANZCR, PhD
Department of Clinical Medicine
Faculty of Medicine and Health Sciences
Macquarie University
2 Technology Place
Sydney, NSW 2109
Australia

E-mail: john.boyages@mq.edu.au

Yi Qian, PhD
Department of Biomedical Science
Faculty of Medicine and Health Sciences
Macquarie University

E-mail: yi.qian@mq.edu.au